Supporting information

A stable silver metallacage with solvatochromic and mechanochromic behaviors for white LED fabrication

Zhixiang Lu, Yi Cheng, Wenwen Fan, Shaoxiong Yang, Xiaolan Liu, Yu Qin, Ruidun Zhao, Liyan Zheng * and Hongbin Zhang *

Key Laboratory of Medicinal Chemistry for Natural Resource (Yunnan University), Ministry of Education, Functional Molecules Analysis and Biotransformation key laboratory of Universities in Yunnan Province, School of Chemical Science and Technology, Yunnan University, Kunming, Yunnan 650091, China.
E-mail: zhengliyan@ynu.edu.cn (L. Zheng), zhanghb@ynu.edu.cn (H. Zhang)

Experimental section

1. Chemicals and materials

Silver nitrate and dimethyl sulfoxide-d_6 were purchased from Sigma Aldrich. N, N-dimethylformamide (DMF), 1,4-dioxane, tetrahydrofuran (THF), acetone and ethyl acetate (EtOAc) were purchased from Energy Chemical. All reagents were of analytical grade and used as received. Ultrapure water was prepared using a Milli-Q water purification system. The blue LED was purchased online.

2. Apparatus

Fluorescence spectra was recorded on a Hitachi High-Technologies Corporation Tokyo Japan 5J2-0004 model F-7000 FL spectrofluorometer. UV-vis absorption was characterized by a UV-vis/NIR spectrophotometer (Shimadzu, Japan). The NMR spectra was recorded with a AVANCEDRX400 NMR spectrometer (Bruker, Germany) operate at 400 MHz. The morphology was characterized with Scanning Electron Microscopy (SEM) (Quanta, FEI) and a JEM 2100 high resolution transmission electron microscope (HRTEM, JEOL, Japan). The Fourier transform infrared (FT-IR) spectra was obtained on a FT-IR spectrophotometer (Thermo Nicolet 365). The height profile was recorded on an Atomic Force Microscope. The measurement of MALDI-TOF using Agilent 6550 iFunnel Q-TOF (QSTAR, USA). Thermogravimetric analysis (TGA) was performed on a NETZSCH STA 449F3 instrument with the heating rate of 10 ℃ min^{-1} under anitrogen atmosphere. X-ray powder diffraction patterns were taken using a D/max-TTR III X-ray diffractometer (Rigaku, Japan) with a scan speed of 0.1 s per step and a step size of 0.01 °. Fluorescent lifetimes were determined on an Edinburgh Analytical Instrument (FLS900 fluorescence spectrometer) with a light-emitting diode lamp and analyzed by

the use of a program for exponential fits. Fluorescence quantum yields measurements were performed on an integrating sphere, with a 280 nm Edinburgh Instruments Ltd. light emitting diode as the excitation source (instrument model no. FLS920). Single crystal fluorescence picture was obtained with a Fluorescent Inverted microscope (Olympus BX53, Olympus, Tokyo, Japan). The crystallographic data collection was performed at 170 K on a Bruker SMART APEX-II CCD area detector using graphite-monochromated Mo-Kα radiation (λ = 0.71073 Å) under anitrogen atmosphere. The data reduction and integration and global unit cell refinements were performed using the INTEGRATE program of the APEX2 software package. Semiempirical absorption corrections were applied using the SCALE program for the area detector. The structures were solved by direct methods and refined using the full-matrix leastsquares methods on F2 using SHELX. CCDC (1894157) contains the supplementary crystallographic data for Ag-TBI-TPE cage. The Zeta potential of cage was detected by NanoBrook 90 plus Zeta (Brookhaven, USA). All the samples analyzed by elemental analysis were microcrystalline powder. One of the elemental analysis methods is determining the content of silver by Inductive Coupled Plasma Emission Spectrometer (ICP) to digest the metallacage, and the other method is measuring the content of organic elements in solid state directly. The organic element analysis of metallacage was analyzed by Thermo Flash 2000.

3. Synthesis

3.1 Synthesis of TBI-TPE.

The synthetic method of TBI-TPE refers to our previous article.

3.2 Synthesis of Ag-TBI-TPE metallacage.

TBI-TPE (20 mg, 0.025 mmol) dissolved in 20 mL methanol solution, $AgNO_3$ (17 mg, 0.1 mmol) dissolved in 100 μL water, and then silver nitrate solution was gradually added to TBI-TPE solution under stirring constantly at room temperature, and bright yellow solid was immediately produced. After 5 minutes, the solid was centrifuged at 14000 rpm for 1 minute, which was washed with methanol and diethyl ether and then was dried under room temperature to provide Ag-TBI-TPE cage as a bright yellow powder in ~98 % yield.

The yellow powder (10 mg) was dissolved in dimethyl sulfoxide (1 mL) and installed in a 10 mL sample bottle without sealing. Then, the bottle was placed in jar containing 30 mL ethyl acetate, and the corresponding yellow transparent single crystal could be obtained after a week static storage, schematic diagram shown in Fig. S1. The single crystal data was submitted to the Cambridge Crystallographic Data Centre (CCDC), and its corresponding number is 1894157.

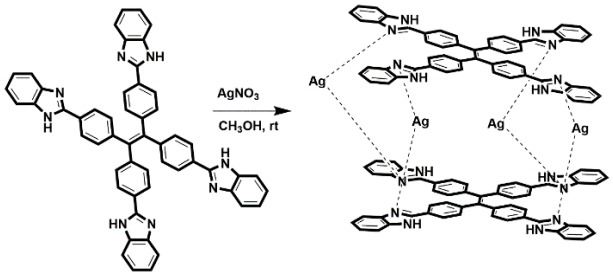

Synthetic route to new Ag-TBI-TPE cage molecule.

4. Fabrication of cage -coated WLED.

By using a dip-coating procedure, the mixture was uniformly dispersed on the surface of a commercially available blue LED (peaking at ~460 nm). This coating process can be easily repeated to ensure uniform and continuous coating of Ag-TBI-TPE cage on the blue LED. Finally, the SCC-coated WLED was obtained and tested at ambient conditions.

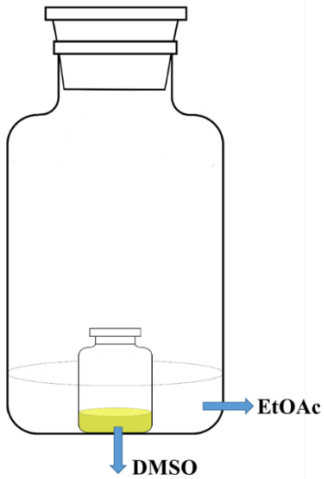

Fig. S1 The schematic diagram of single crystal was obtained by slow diffusion method.

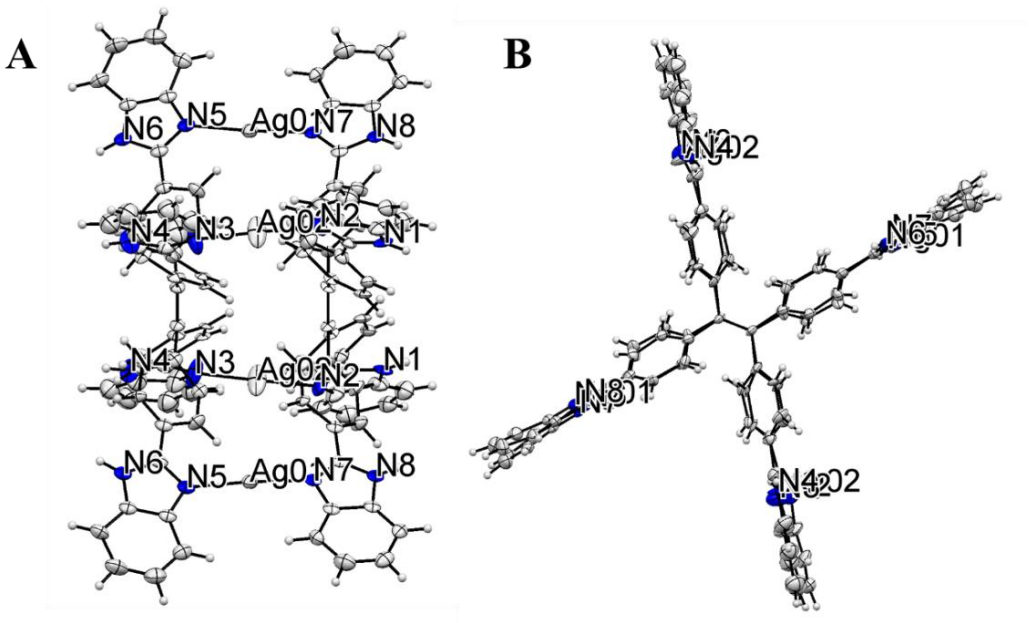

Fig. S2 (A)The single crystal X-ray structure of new Ag-TBI-TPE cage view from a direction; (B)The single crystal X-ray structure of new Ag-TBI-TPE cage view from b direction; C light grey, N blue, Ag grey, H light grey. All of the NO_3^- and DMSO were omitted for clarity.

Table S1 The content of Ag in the Ag–TBI–TPE cage.

Sample	Theoretical content (%)	Test content (%)	Error (%)
1	16.571	17.393	4.960
2	16.571	17.273	4.236
3	16.571	17.063	2.969

Table S2 The content of element analysis in the Ag–TBI–TPE cage.

Element Analysis	C (%)	N (%)	O (%)
Test content	53.580	11.361	9.998
Theoretical content	53.459	10.753	10.446
Error (%)	0.226	5.750	-4.289

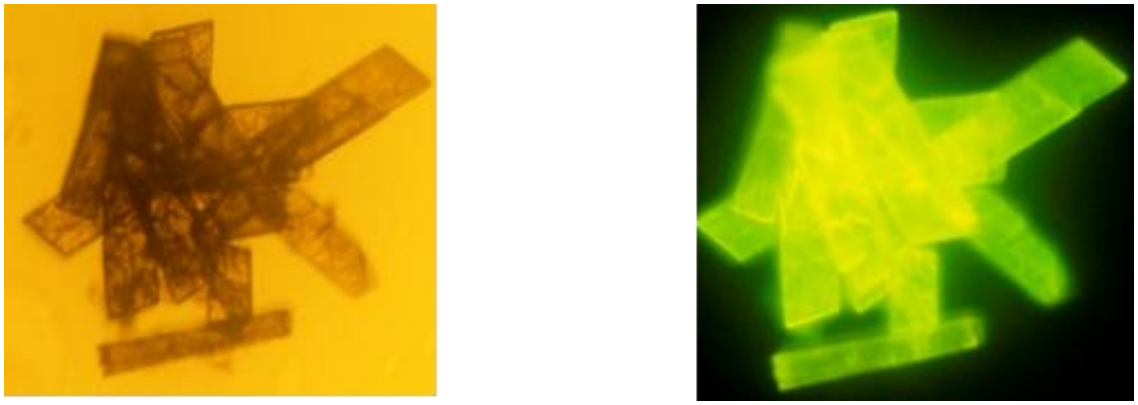

Fig. S3 Single crystal picture of Ag-TBI-TPE cage under the bright field (left) and fluorescent picture under fluorescent inverted microscope(Ex=365 nm right).

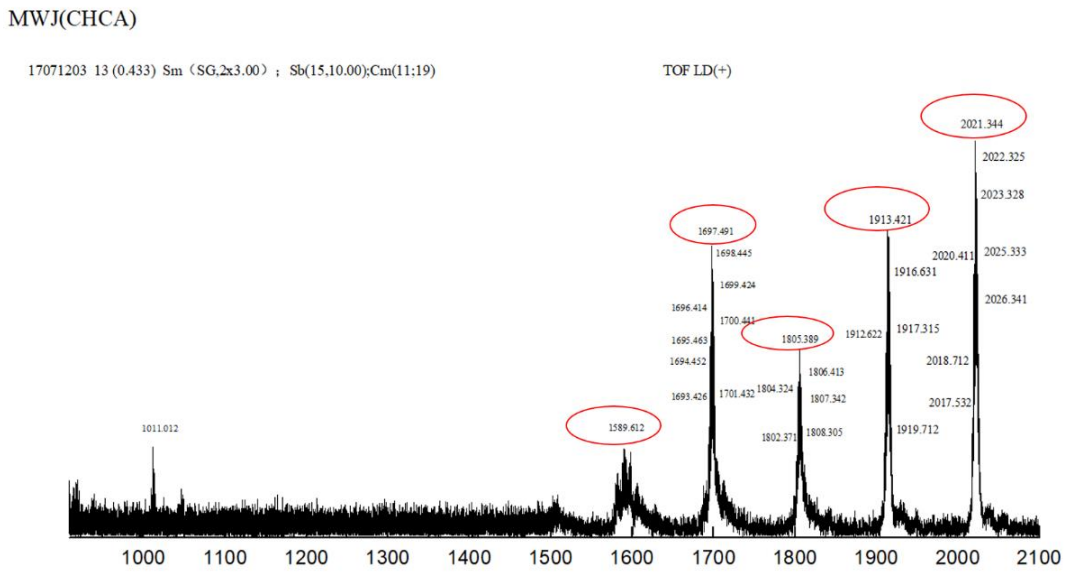

Fig. S4 MALDI-TOF spectra of the Ag–TBI–TPE cage.

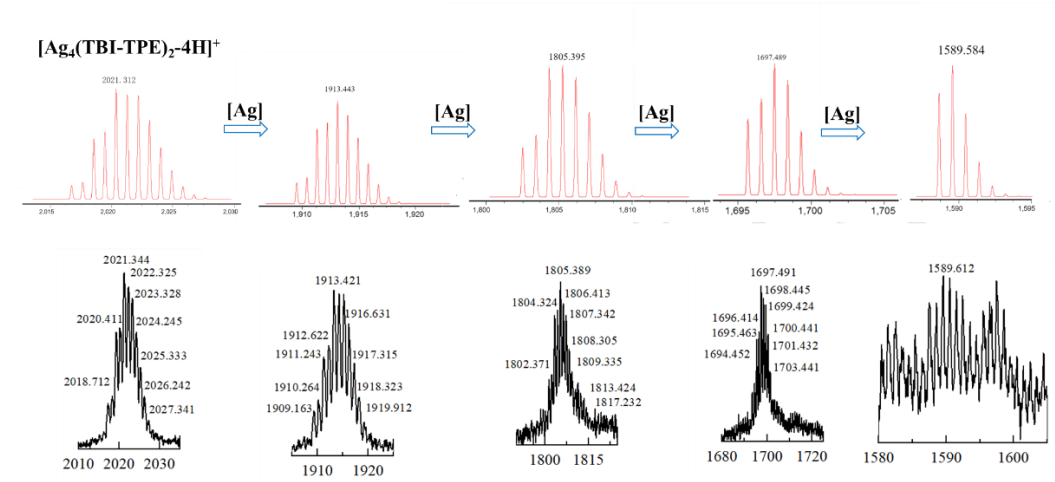

Fig. S5 Calculated (top) and experimental (bottom) MALDI-TOF Spectra of the Ag–TBI–TPE cage.

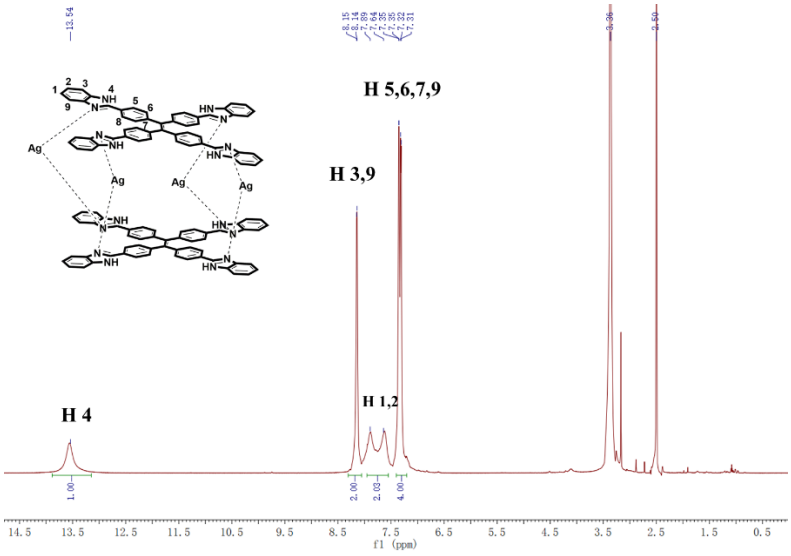

Fig. S6 ^{1}H NMR spectra of compound Ag–TBI–TPE cage in d_6-DMSO.

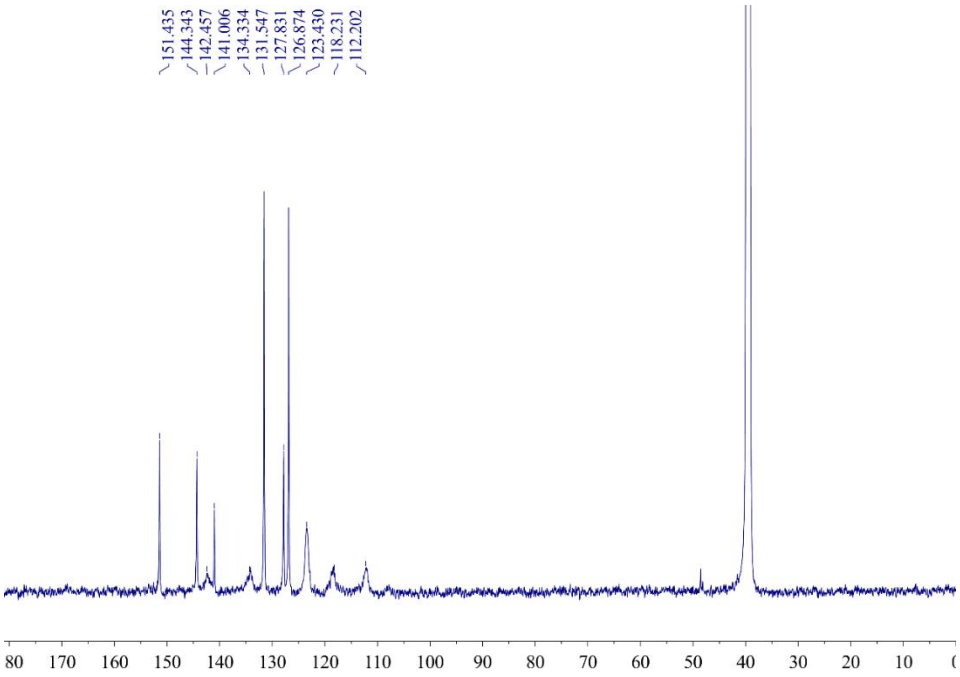

Fig. S7 ^{13}C NMR spectrum of compound Ag–TBI–TPE cage in d_6-DMSO.

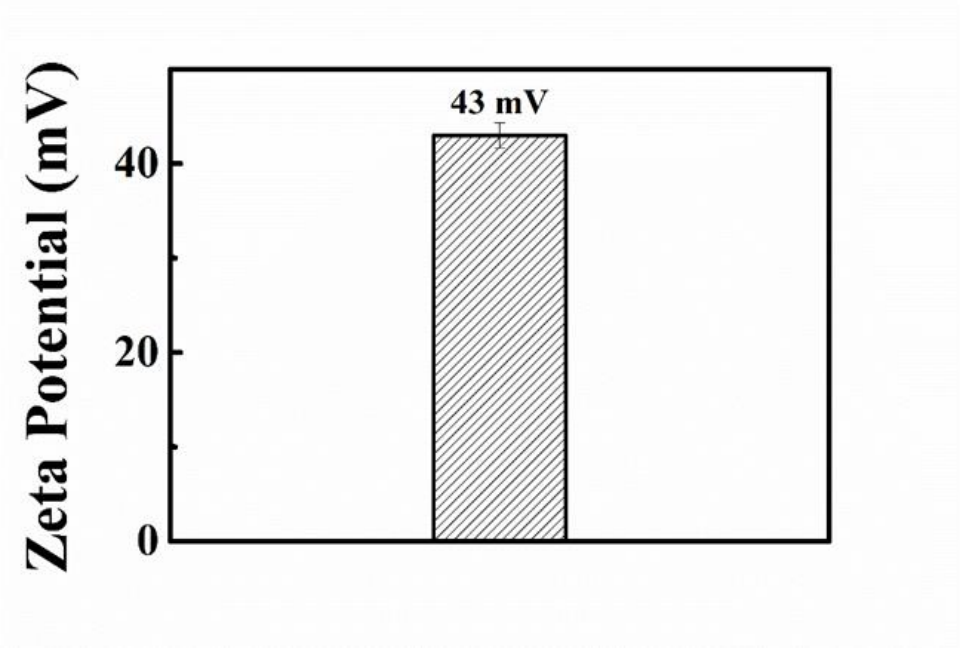

Fig. S8 Zeta potentials of Ag- TBI-TPE cage in water.

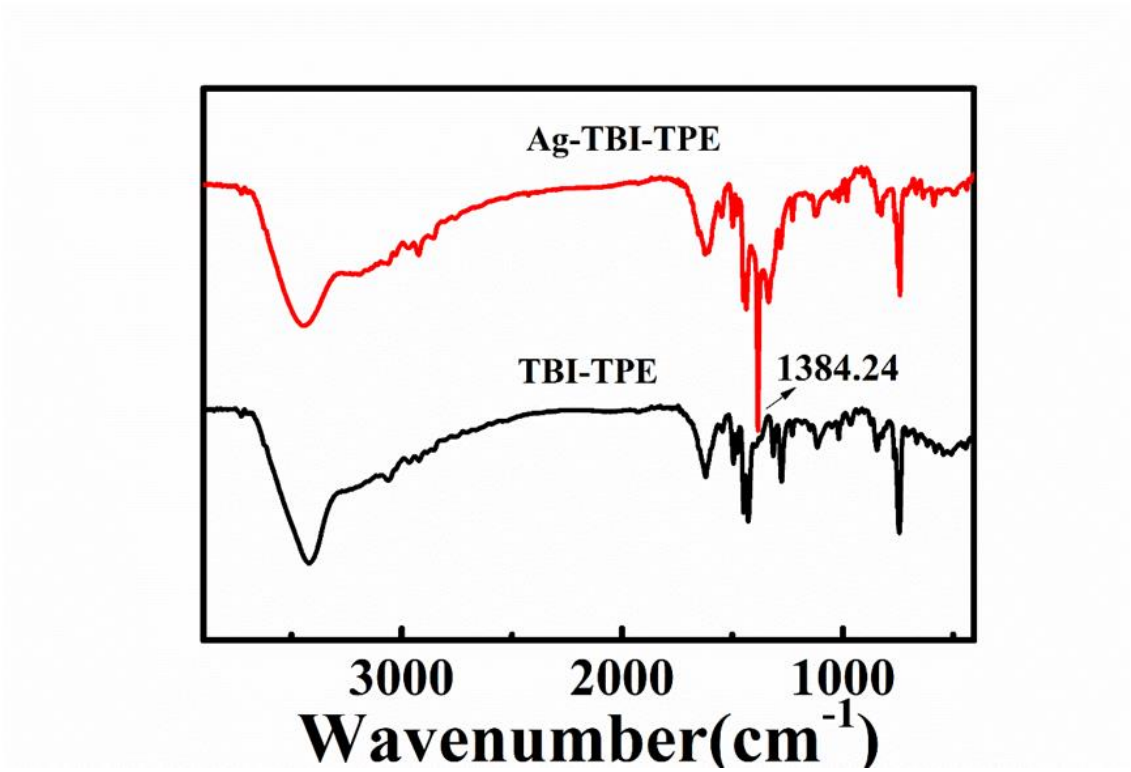

Fig. S9 The FTIR spectrum of compound Ag–TBI–TPE cage and TBI–TPE.

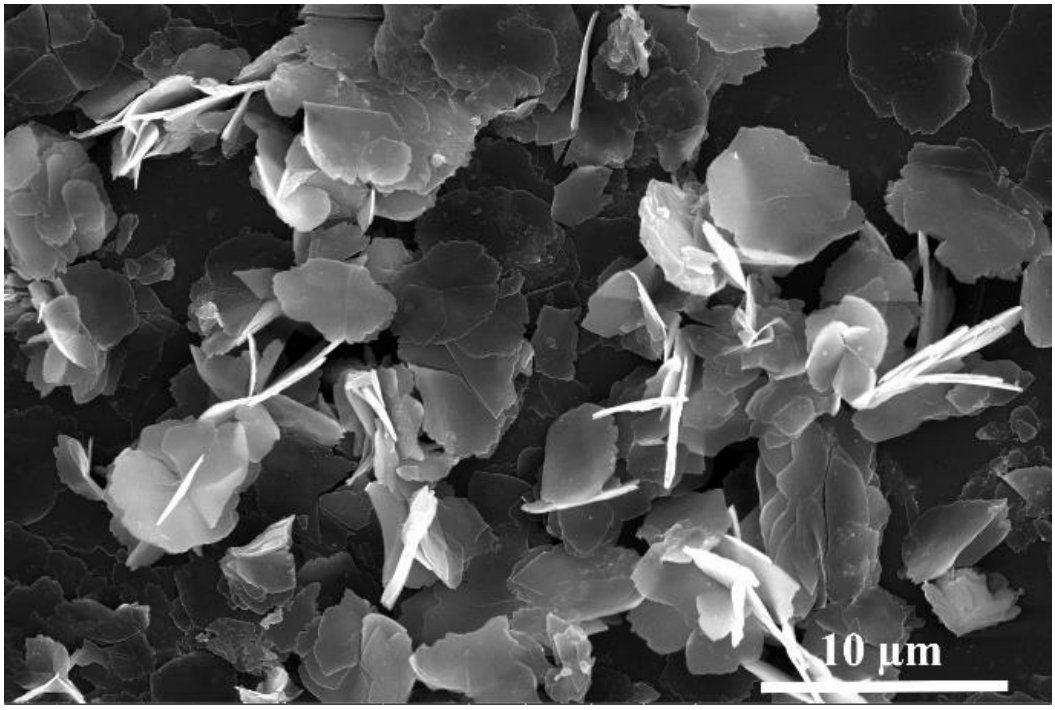

Fig. S10 SEM image of Ag–TBI–TPE cage.

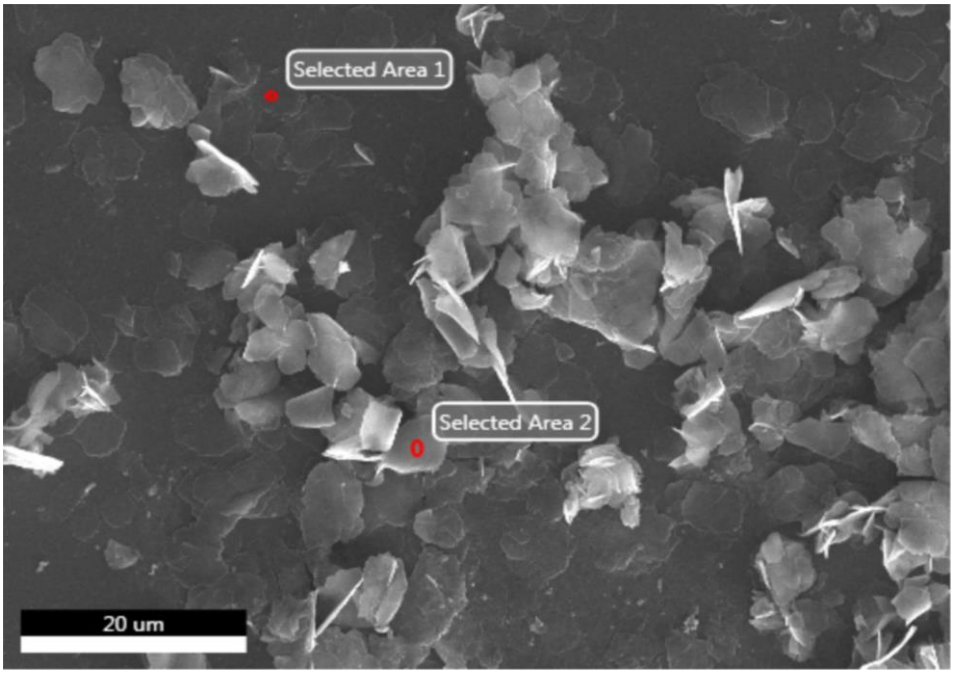

Fig. S11 SEM mage of Ag–TBI–TPE cage.

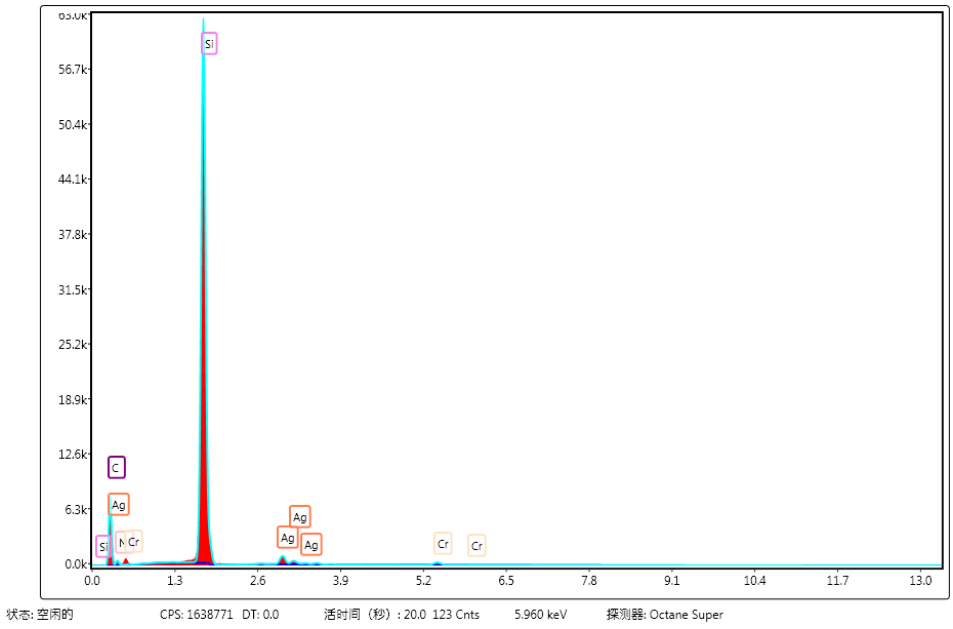

Fig. S12 Energy Dispersive X-Ray Spectroscopy of Ag–TBI–TPE cage about selected area 1 during SEM measurement.

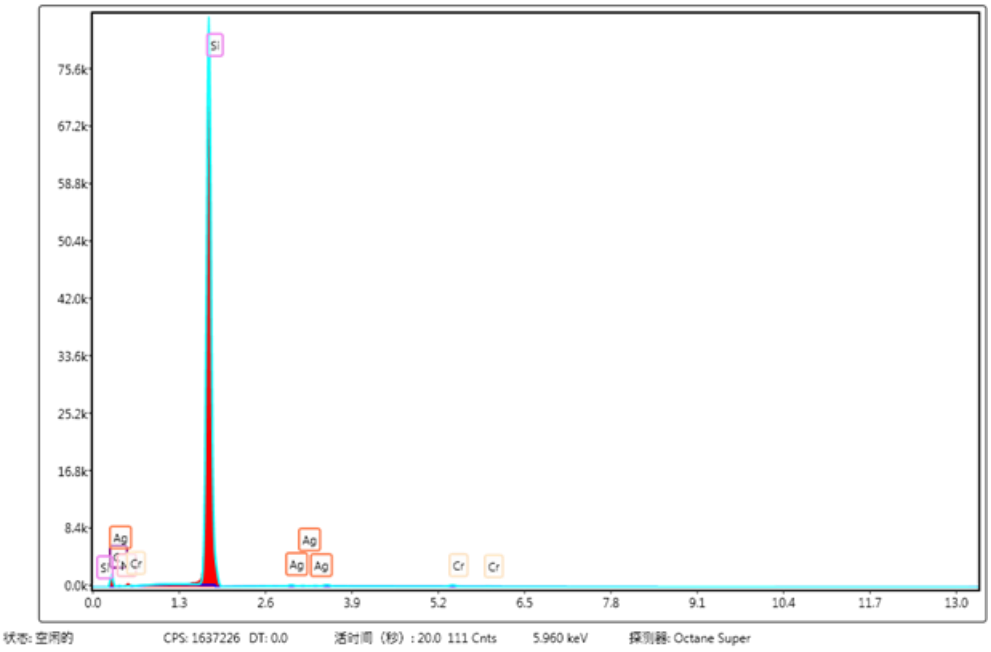

Fig. S13 Energy Dispersive X-Ray Spectroscopy of Ag–TBI–TPE cage about selected area 2 during SEM measurement.

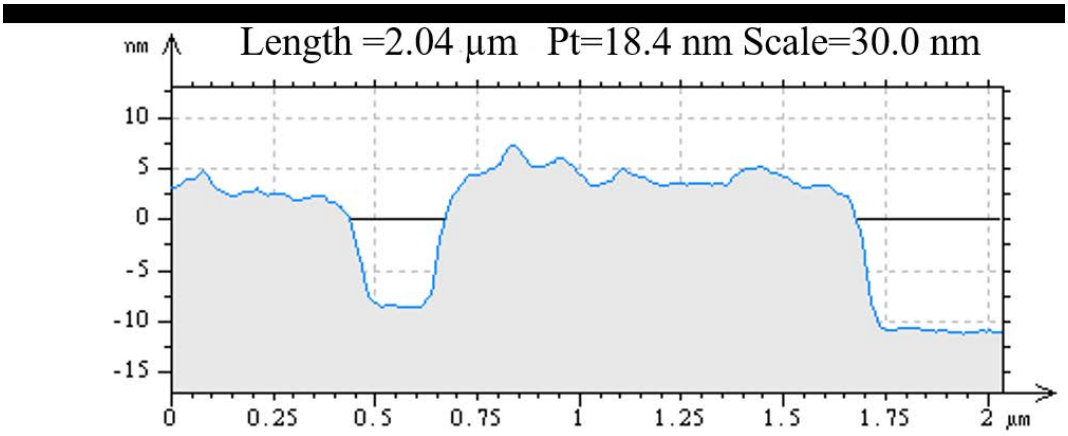

Fig. S14 Selected AFM height profiles of Ag–TBI–TPE cage.

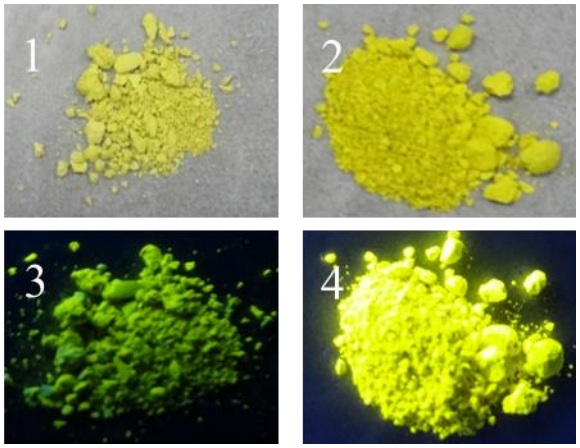

Fig. S15 Photographs of TBI–TPE (1) and Ag–TBI–TPE cage (2) solid powder under white light, photographs of TBI–TPE(3) and Ag–TBI–TPE cage (4) solid powder under 365 nm UV light.

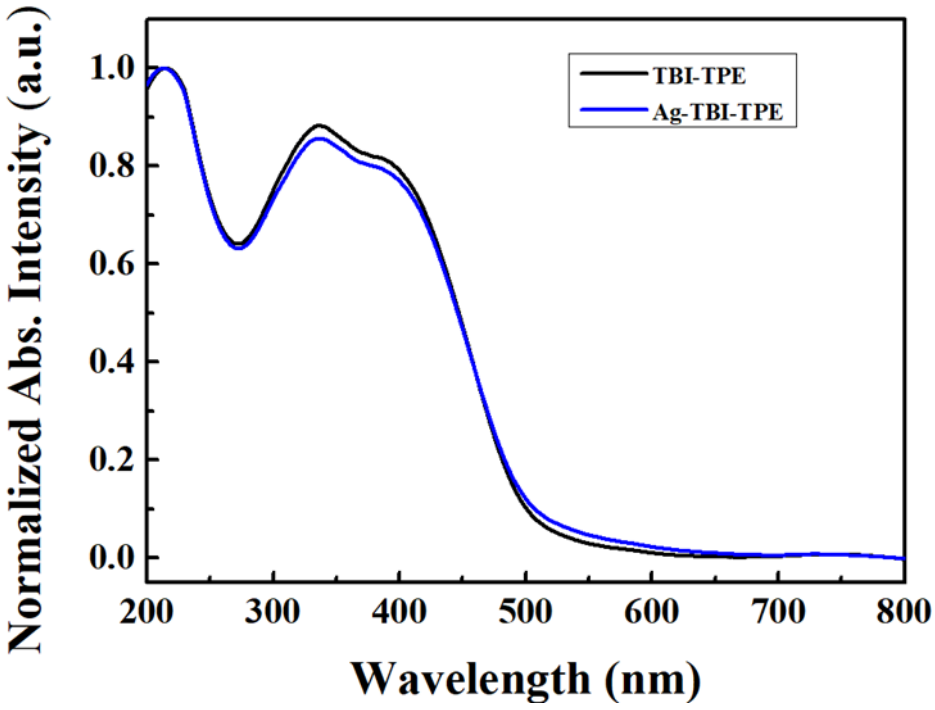

Fig. S16 Solid UV absorption of TBI–TPE and Ag–TBI–TPE cage.

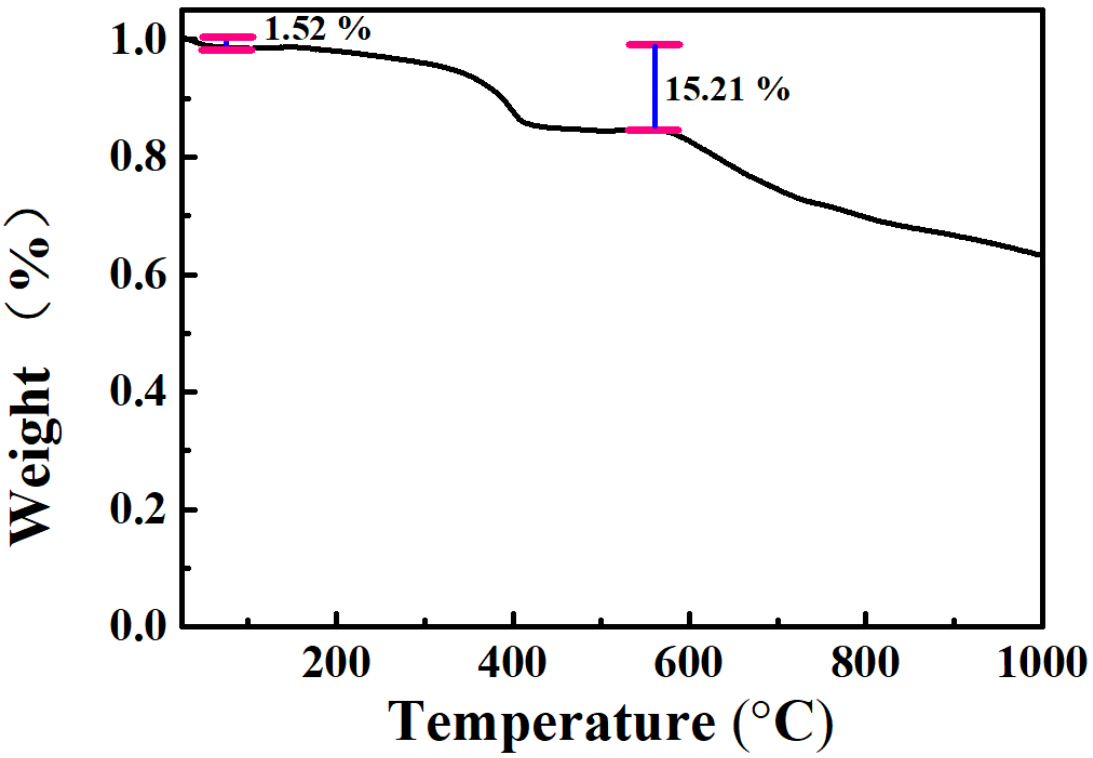

Fig. S17 Thermogravimetric analysis (TGA) of Ag–TBI–TPE cage under N_2 atmosphere.

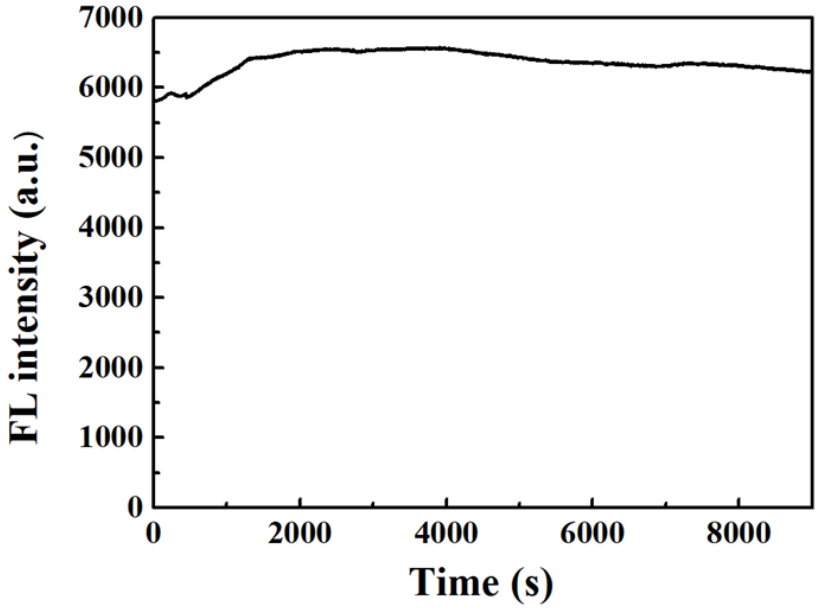

Fig. S18 Fluorescent time curve of Ag–TBI–TPE cage (concentration: 50 μM) in DMF, λ_{ex}=410 nm.

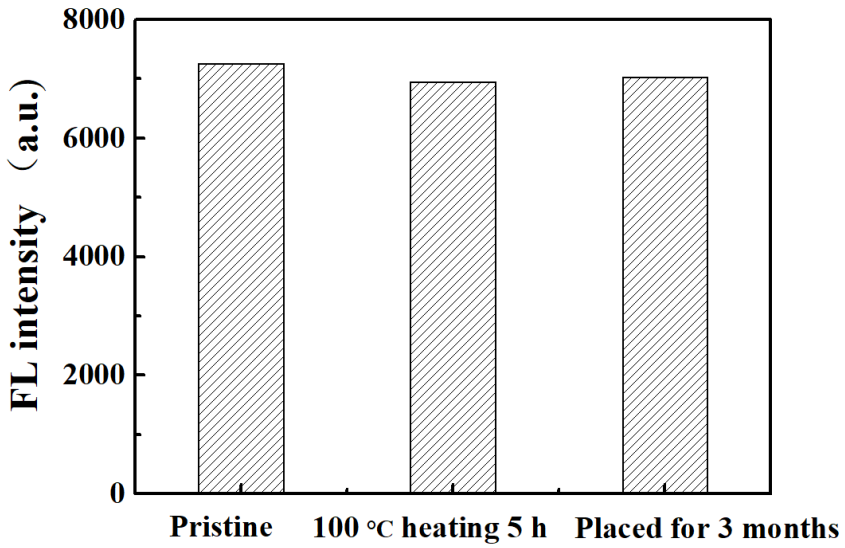

Fig. S19 Solid fluorescence spectrum of Ag–TBI–TPE cage under different conditions.

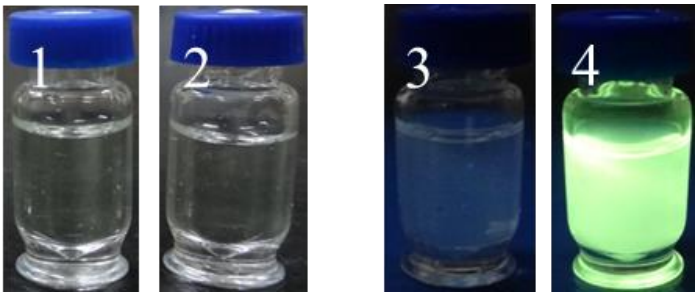

Fig. S20 Photographs of TBI–TPE (1) and Ag–TBI–TPE cage (2) dissolved in DMF under white light, photographs of TBI–TPE (3) and Ag–TBI–TPE cage (4) under 365 nm UV light.

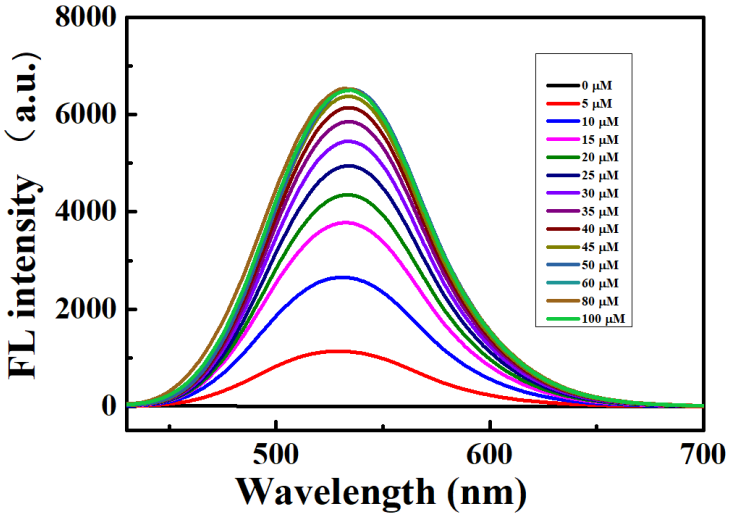

Fig. S21 Fluorescent spectra of Ag - TBI - TPE at different concentrations in DMF.

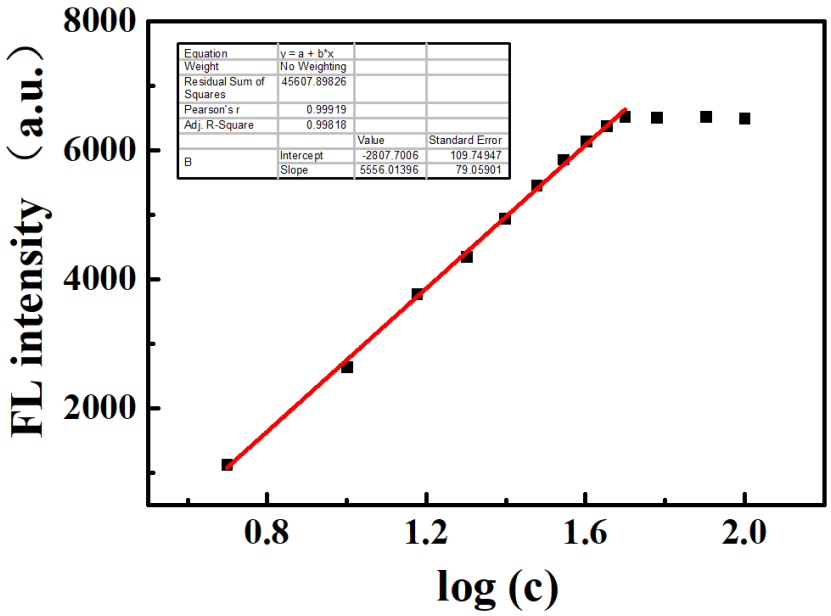

Fig. S22 Variation of the fluorescent intensity at 530 nm of Ag–TBI–TPE cage with gradual increase concentration (from 5 to 50 μM) in DMF, λ_{ex}=410 nm.

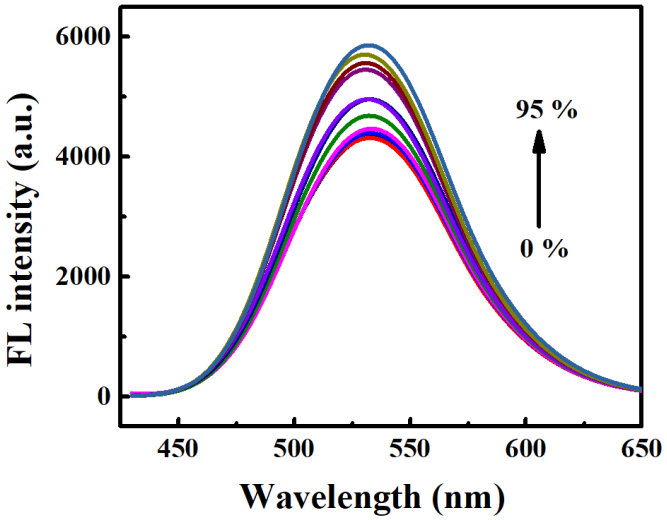

Fig. S23 Fluorescent intensity spectra versus water fraction of Ag–TBI–TPE cage (concentration: 50 μM) in mixtures of DMF/water with different water fractions (from 0 to 95 %).

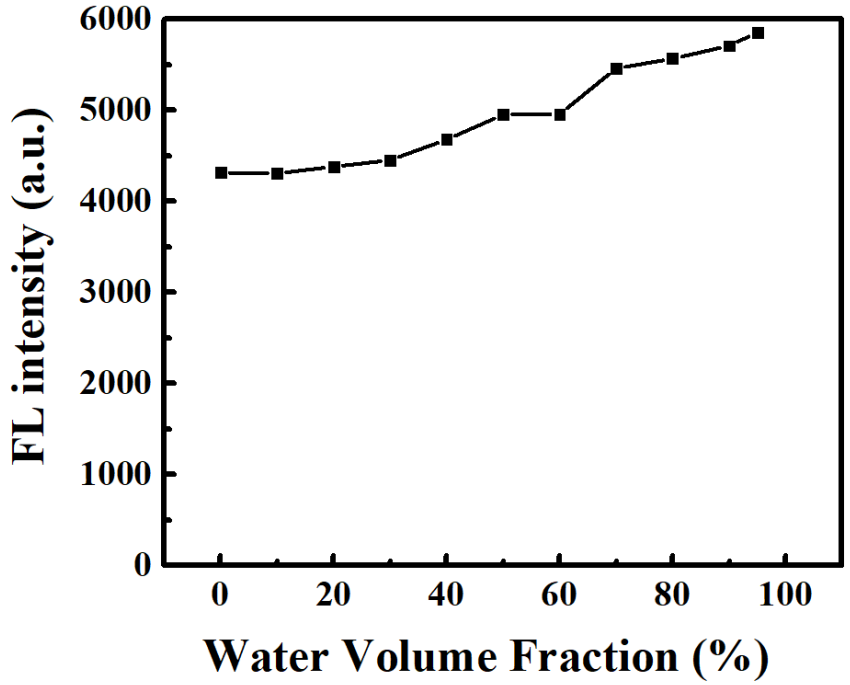

Fig. S24 Plots of fluorescent intensity versus water fraction of Ag–TBI–TPE cage (concentration: 50 μM) in mixtures of DMF/water with different water fractions (from 0 to 95 %).

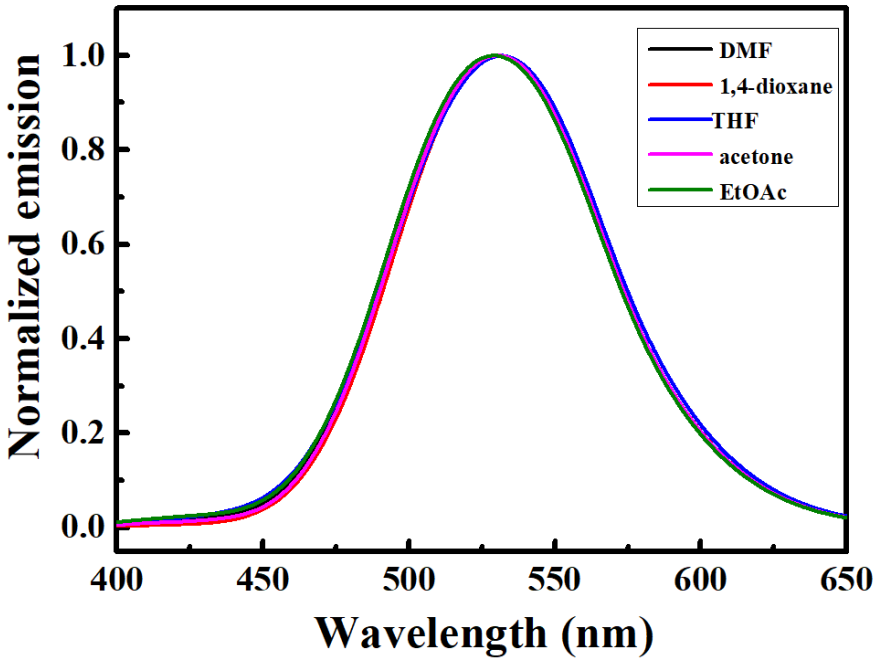

Fig. S25 Fluorescent spectrum of TBI–TPE in different organic solvent.

Table S3 Spectroscopic data for TBI–TPE and Ag–TBI–TPE cage in different organic solvent.

Name	State	E_m (nm)	Φ_f (%)	τ (ns)	$k_r/10^8(s^{-1})$	$k_{nr}/10^8(s^{-1})$
TBI–TPE	DMF	530	0.98	0.58	0.17	17.07
	1,4-dioxane	530	0.94	0.53	0.18	18.67
	THF	530	0.89	0.55	0.16	18.02
	acetone	530	0.85	0.43	0.20	23.06
	EtOAC	530	0.95	0.80	0.12	12.38
Ag–TBI–TPE cage	DMF	530	34.41	3.84	0.89	1.71
	1,4-dioxane	463	42.62	1.45	2.94	3.96
	THF	495	25.77	2.37	1.09	3.13
	acetone	525	29.55	2.64	1.12	2.67
	EtOAC	515	16.74	2.06	0.81	4.04

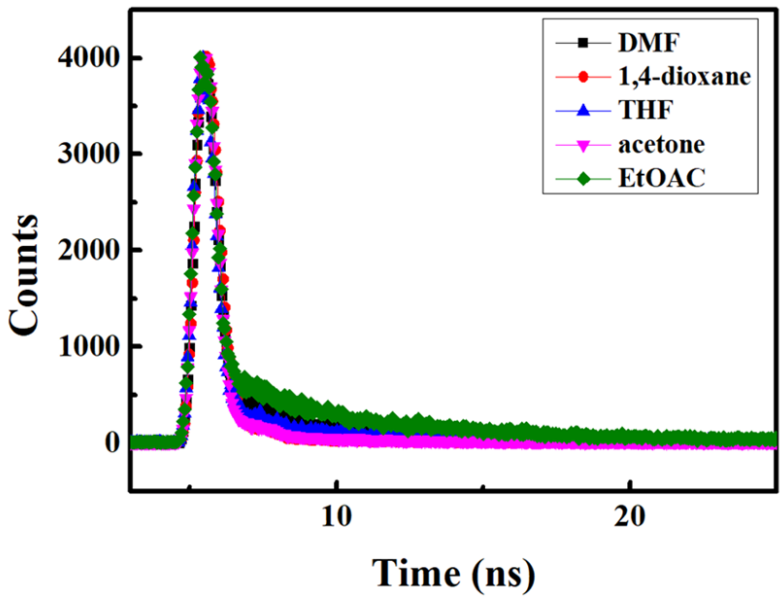

Fig. S26 Fluorescence lifetime of TBI-TPE in different organic solution.

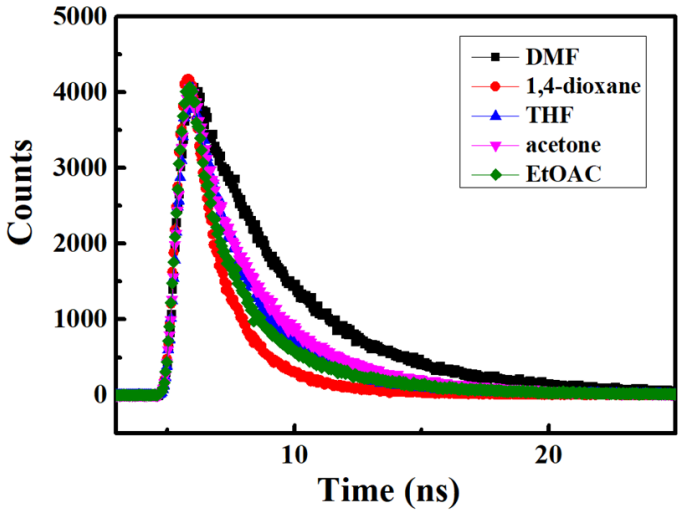

Fig. S27 Fluorescence lifetime of Ag-TBI-TPE cage in different organic solution.

Table S4 Spectroscopic data for TBI–TPE and Ag–TBI–TPE cage.

Name	State	E_m(nm)	Φ_f (%)	τ (ns)	$k_r/10^8(s^{-1})$	$k_{nr}/10^8(s^{-1})$
TBI–TPE	**solid**	**542**	**2.31**	**1.79**	**0.13**	**5.46**
Ag–TBI –TPE cage	**solid**	**543**	**12.46**	**2.14**	**0.58**	**4.09**
Ag–TBI–TPE grinding	**solid**	**543**	**2.25**	**2.09**	**0.12**	**5.21**

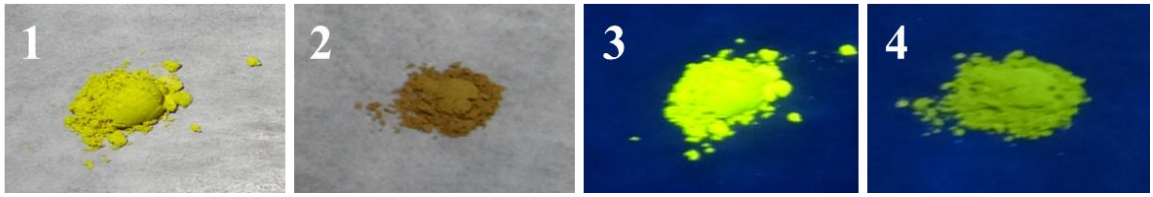

Fig. S28 Photographs of Ag–TBI–TPE cage in different treatments under white light (1. pristine; 2. grinding), photographs of Ag–TBI–TPE cage in different treatments under 365 nm UV light (3. pristine; 4. grinding).

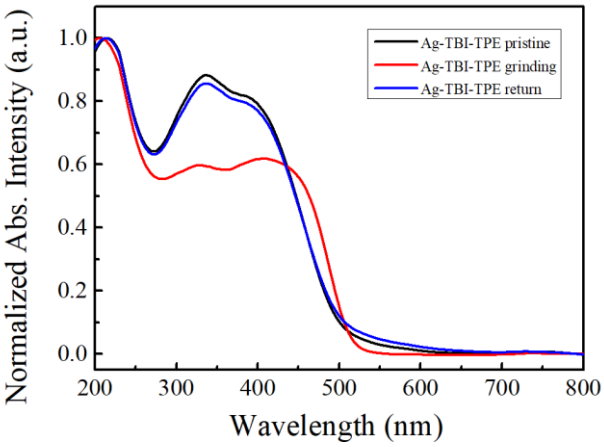

Fig. S29 Solid UV absorption of Ag–TBI–TPE cage in different treatments.

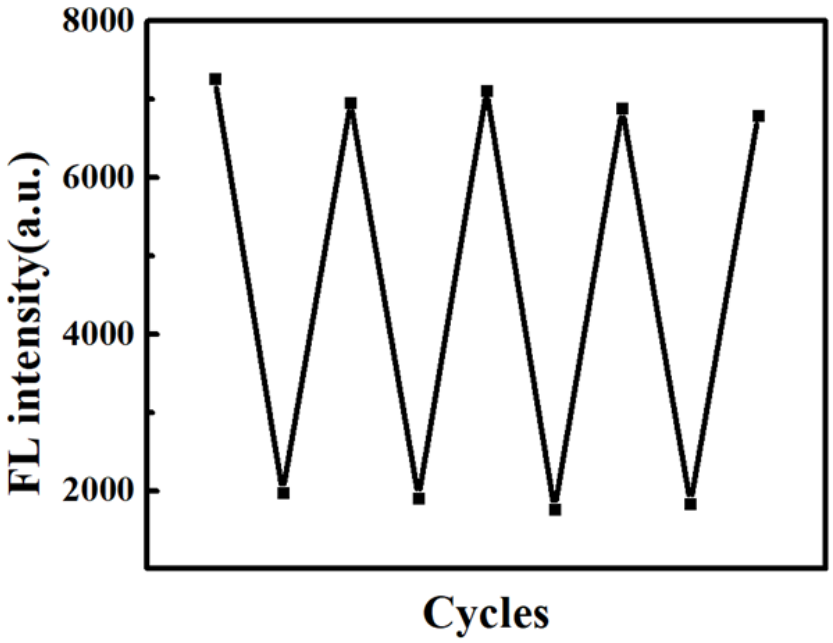

Fig. S30 Reversible switching of emission of Ag–TBI–TPE cage.

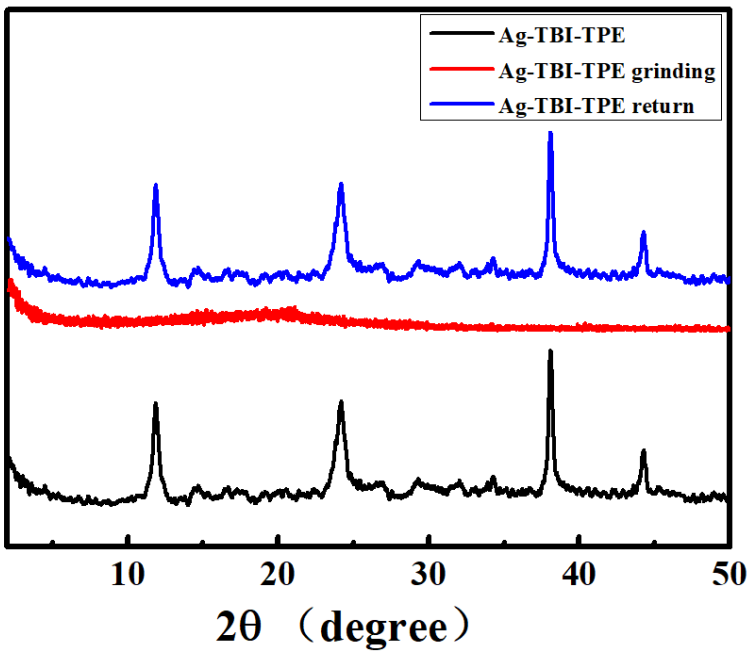

Fig. S31 XRD patterns of Ag–TBI–TPE cage pristine, grinding, return.

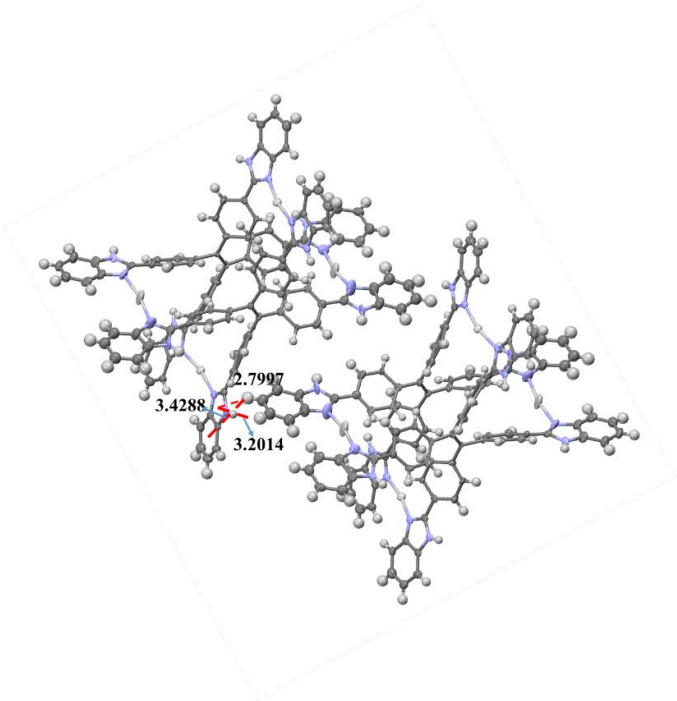

Fig. S32 Intermolecular interactions of Ag–TBI–TPE cage.

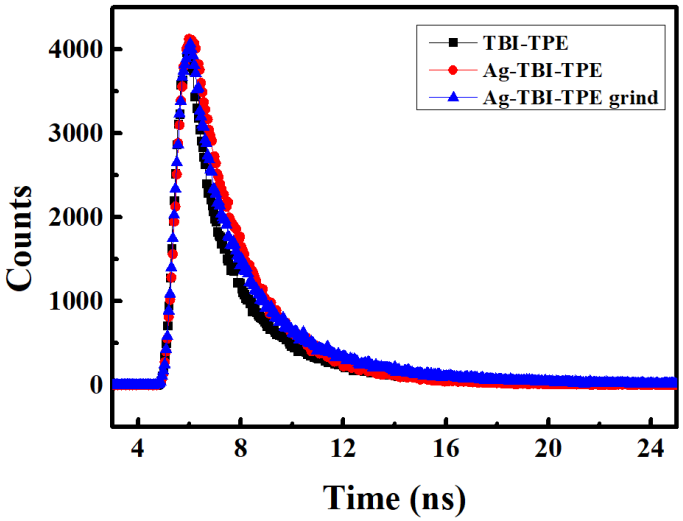

Fig. S33 Fluorescence lifetime of Ag-TBI-TPE cage in different treatments.

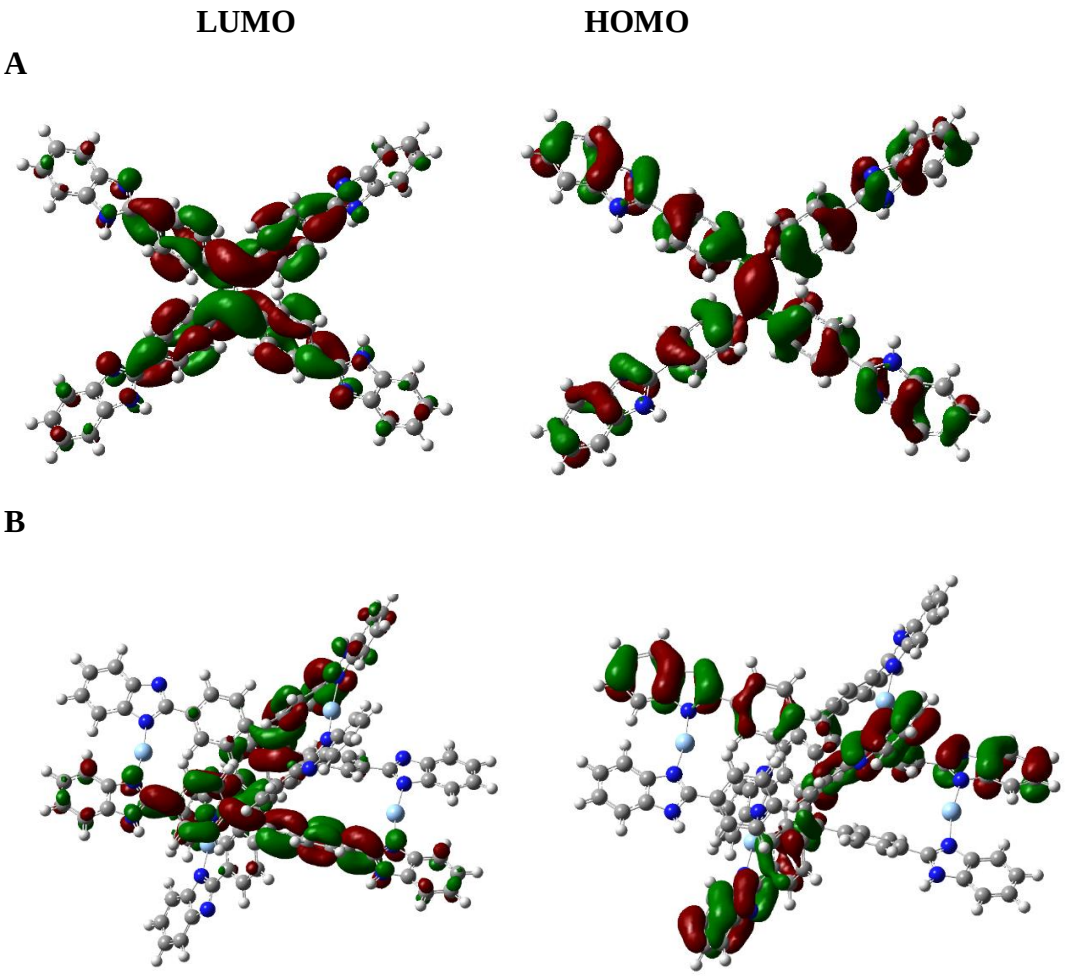

Fig. S34 LUMO, HOMO and electron cloud distributions of TBI–TPE(A) and Ag–TBI–TPE cage(B).

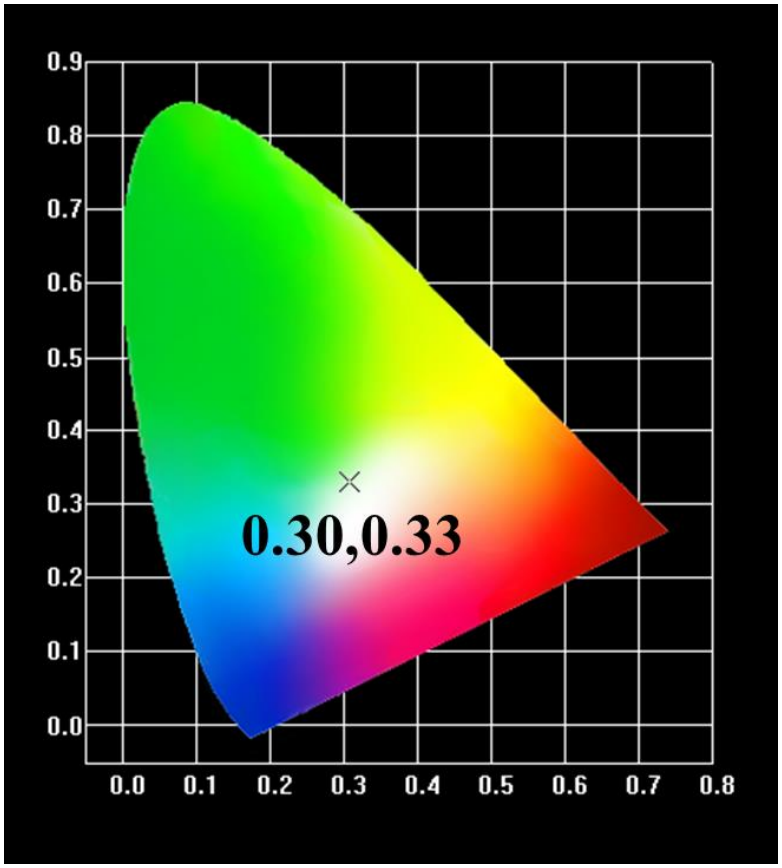

Fig. S35 CIE chromaticity coordinates of the painted LED at ambient condition for 10 days.